JOURNAL OF MATERIALS SCIENCE **36** (2001) 2427–2433

Hardness and elastic properties of Bi_2O_3-based glasses

T. WATANABE, K. MURATSUBAKI, Y. BENINO, H. SAITOH, T. KOMATSU*
Department of Chemistry, Nagaoka University of Technology, Nagaoka 940-2188, Japan
E-mail: komatsu@chem.nagaokaut.ac.jp

The hardness and elastic properties of $20PbO \cdot xBi_2O_3 \cdot (80-x)B_2O_3$ glasses with $x = 20$–60 were evaluated through usual Vickers indentation and nanoindentation tests. The glass transition temperature ($T_g = 295$–421°C), Vickers hardness ($H_v = 2.9$–4.5 GPa), true hardness ($H = 1.5$–3.8 GPa) and Young's modulus ($E = 24.4$–72.6 GPa) decreased monotonously with increasing Bi_2O_3 content. This compositional trend demonstrates that the strength of Bi–O chemical bonds in these glasses is considerably weak compared with B–O bonds and plastic deformations under indentation loading occur easily. The elastic recovery after unloading was about 45% for the glasses with $x = 20$–50, and the Poisson's ratio was 0.27 for the glass with $x = 20$. The fracture toughness was evaluated to be 0.37–0.88 $MPam^{1/2}$ from the values of H_v and E, and it was proposed that not only weak Bi–O bonds but also boron coordination polyhedra (BO_3 or BO_4) and their arrangements affect on crack formation. From the temperature dependence of Vickers hardness up to the glass transition region, it was suggested that the glasses with high Bi_2O_3 contents belong to the category to fragile glass-forming liquids.

1. Introduction

Since the first report by Dumbaugh [1] on bismuth oxide (Bi_2O_3) based glasses being thermally stable against crystallization and showing high refractive indices and excellent infrared transparencies, so many studies on structure and optical properties of Bi_2O_3-based glasses such as PbO-Bi_2O_3-B_2O_3 and PbO-Ga_2O_3-Bi_2O_3 have been carried out. For example, it has been found that glasses containing Bi_2O_3 exhibit extremely large third-order nonlinear optical susceptibilities $\chi^{(3)}$ of the order 10^{-12} esu [2–4]. It is also known that Bi_2O_3-based glasses are excellent host materials for rare-earth doping to get efficient fluorescence emissions because of their low phonon energies (i.e. small multi-phonon relaxations) [5, 6]. For technical applications of such attractive Bi_2O_3-based glasses, it is obvious that an understanding of mechanical and elastic properties is necessary, because generally poor mechanical and elastic properties of glasses and ceramics limit their use in many applications. To our best knowledge, however, the study of mechanical and elastic properties such as hardness, Young's modulus and fracture toughness in Bi_2O_3-based glasses is scarce [7, 8].

Glass undergoes both compression and shear during the process of deformation in indentation test, and consequently the observed deformation comprises elastic deformation, plastic flow and densification [9–13]. It is recognized that so-called normal glasses such as soda-lime silicate glasses deform largely by a shear-dominated flow process, which is necessary reconstructive in the bond configuration, i.e. bonds must be continuously broken and remade with new neighbors. It is, therefore, obvious that glasses having weak bond strengths among constituents atoms and small atom packing densities (i.e. more open structure) show low mechanical and elastic properties such as small Young's modulus [14]. In this paper, we focus our attention on PbO-Bi_2O_3-B_2O_3 glasses, because these glasses with a wide content range of Bi_2O_3 are available through a conventional melt-quenching method and show excellent optical properties [4]. Further, their network structure has been examined in detail [4]. The Vickers hardness and fracture toughness at room temperature of PbO-Bi_2O_3-B_2O_3 glasses were evaluated through usual Vickers indentation tests, and the Young's modulus and the fraction of elastic recovery during unloading were determined from indentation load-unload/displacement experiments, i.e. so-called nanoindentation tests. The temperature dependence of Vickers hardness of some glasses in the range from room temperature to glass transition temperature was also measured. Such information would be valuable, when Bi_2O_3-based glasses are used under high power laser irradiations. It should be pointed out that the study of the temperature dependence of hardness for glass has been limited to a few papers [15–17]. In this study, it has been demonstrated that the strength of Bi–O chemical bonds is considerably weak compared with B–O bonds, giving the decreases in Vickers hardness and Young's modulus with Bi_2O_3 content and also showing a fragile character in the glass transition region.

* Author to whom all correspondence should be addressed.

2. Experimental

The nominal compositions examined in the present study are $20PbO \cdot xBi_2O_3$ $(80-x)B_2O_3$ with $x = 20$, 30, 40, 50 and 60. The glasses were prepared using a conventional melt-quenching method. Commercial powders of reagent grade PbO, Bi_2O_3 and B_2O_3 were mixed and melted in a platinum crucible at 800°C for 30 min in an electric furnace. After melting, the melt was poured onto an iron plate heated to 150°C. Glass transition temperatures, T_g, were determined by using differential thermal analysis (DTA) at a heating rate of 10 K min^{-1}. Densities, d, were determined by the Archimedes method using kerosene as the immersion liquid. The glasses having mirror surface were prepared by mechanical polishing with lapping films containing 3.0 μm Al_2O_3 powders and then the glasses with a thickness of about 1.5 mm were annealed at a temperature of $T_g + 10$°C for 10 min to eliminate internal stress in the glasses. Such well-polished glasses were used for indentation tests.

Vickers hardness, H_v, at room temperature was measured using Akashi HM-114 in air (relative humidity was 64%). The applied loads were in the range of 245 mN–9.8 N, and the time of loading was 15 s. The temperature dependence of Vickers hardness of the glasses was measured using a high temperature-type equipment of Nikon QM-2 in the temperature range from room temperature to around T_g in a vaccum of 1.33×10^{-3} Pa. The hardness, H, Young's modulus, E, and the fraction of elastic recovery during unloading were also evaluated using a Fischer scope H100V ultralow-load microhardness indenter designed by Fischer Co. at room temperature. A diamond Vickers indenter tip was used with a geometrical correction procedure for accurate calculation of hardness. The load was applied to 490 mN over a period of 30 s and then the applied load was decreased to 0 mN over a period of 30 s. Measurements for each sample were carried out ten times under the same measuring condition, and the mean values of H and E were estimated. In this paper, the hardness H evaluated from the above indentation load-unload/displacement experiments are called "true hardness", in order to distinguish this hardness from usual Vickers hardness H_v. The Poisson's ratio was measured from a cube resonance method with the frequencies of 0.2–1 MHz, in which the sample size was $3 \times 3 \times 3$ mm [18, 19].

3. Results and discussion

3.1. Properties of glasses

The values of glass transition temperature T_g and density d for $20PbO \cdot xBi_2O_3$ $(80-x)B_2O_3$ glasses are given in Table I. The glass transition temperature decreases rapidly from 421°C for the glass with $x = 20$ to 295°C for the glass with $x = 60$ with the substitution of Bi_2O_3 for B_2O_3. The density increases steeply from 5.77 to 8.17 g cm^{-3} with increasing Bi_2O_3 content. The mean atomic volumes V_m were calculated from the densities and chemical compositions, and their values are given in Table I. It is seen that they increase from 7.07 to 9.41 cm^3 g-$atom^{-1}$ with increasing Bi_2O_3 content, implying that the glasses change toward more open structure with the substitution of Bi_2O_3 for B_2O_3. Stehle *et al.* [20] proposed that the glass structure in bismuth borate glasses becomes more and more open as the bismuth concentration increases. The thermal expansion coefficient of $\alpha = 10.4 \times 10^{-6}$ K^{-1} for the glass with 60 mol% Bi_2O_3 content is larger than that for the glass with 40 mol% Bi_2O_3 content ($\alpha = 8.9 \times 10^{-6}$ K^{-1}).

TABLE I Values of glass transition temperature T_g, density d and mean atomic volume V_m for $20PbO \cdot xBi_2O_3 \cdot (80-x)B_2O_3$ glasses. The data for $15Na_2O \cdot 15ZnO \cdot 70TeO_2$ (tellurite) and $14Na_2O \cdot 13CaO \cdot 73SiO_2$ (soda-lime) glasses are also shown [17]

x (mol%)	T_g (°C)	d (gcm^{-3})	V_m (cm^3g-$atom^{-1}$)
20	421	5.77	7.07
30	387	6.55	7.61
40	359	7.22	8.15
50	328	7.75	8.75
60	295	8.17	9.41
tellurite	264	4.94	9.46
soda-lime	555	2.50	8.27

Miyaji and Sakka [21] reported that Bi^{3+} ions in PbO-Bi_2O_3-Ga_2O_3 glasses are present in BiO_6 distorted octahedral. Janewicz *et al.* [22] proposed that lead ions in PbO-Bi_2O_3-Ga_2O_3 glasses are present as PbO_3 trigonal and/or PbO_4 pyramids. Terashima *et al.* [4] examined the boron atom coordination state in PbO-B_2O_3 and Bi_2O_3-B_2O_3 glasses from Raman and ^{11}B NMR spectroscopies and proposed that the fraction of BO_4 groups increases with increasing PbO or Bi_2O_3 content (up to 50 mol%) and then decreases with further PbO or Bi_2O_3 content (over 50 mol%). It has been considered that in borate glasses with less than 50 mol% B_2O_3, meta-, pyro-and ortho-borate structures are formed [4, 23]. Terashima *et al.* [4] also showed that the coordination number of Bi^{3+}, however, remains unchanged. From various studies on the structure of Bi_2O_3-based glasses, it is obvious that Bi^{3+} ions act as network former in PbO-Bi_2O_3-B_2O_3 glasses. It is, therefore, reasonable to assume that the connectivity of –B–O–B– network bonds decreases and other network bonds such as –B–O–Bi– and –Bi–O–Bi– are formed with the substitution of Bi_2O_3 for B_2O_3. And, further, the BO_3 (two-dimensional) and BO_4 (three-dimensional) ratio changes and chain-type metaborate groups (one-dimensional) are formed as B_2O_3 content decreases. The low T_g values and the monotonous compositional dependence of T_g given in Table I indicate that the strength of Bi–O chemical bonds in PbO-Bi_2O_3-B_2O_3 glasses is considerably weak compared with B–O bonds. The change in the dimension of boron-oxygen coordination also might contribute to the T_g value.

3.2. Vickers hardness, fracture toughness and brittleness at room temperature

From deformation-fracture patterns in Vickers indenter tests, the values of Vickers hardness, H_v, for the

TABLE II Values of Vickers hardness H_v, Young's modulus E, fracture toughness K_c, brittleness B, elastic recovery ER, and true hardness H estimated from nanoindentation tests for $20PbO \cdot xBi_2O_3 \cdot (80-x)B_2O_3$ glasses. The data for $15Na_2O \cdot 15ZnO \cdot 70TeO_2$ (tellurite) and $14Na_2O \cdot 13CaO \cdot 73SiO_2$ (soda-lime) glasses are also shown [17]

x (mol%)	H_v (GPa)	E (GPa)	K_c (MPam$^{1/2}$)	B (μm$^{-1/2}$)	ER (%)	H (GPa)
20	4.5	72.6	0.88	5.1	45.1	3.8
30	4.3	69.8	0.66	6.5	43.8	3.6
40	3.9	53.9	0.45	8.6	45.7	2.9
50	3.4	45.0	0.46	7.4	43.4	2.4
60	2.9	24.4	0.37	7.8	54.9	1.5
tellurite	2.5		~0.23	~10		
soda-lime	6.0	~70	~0.75	~8		

$20PbO \cdot xBi_2O_3$ $(80-x)B_2O_3$ glasses were evaluated using Equation 1:

$$H_v = \frac{P}{\alpha_0 a^2} \tag{1}$$

where P is an applied load, a is a characteristic indentation diagonal and α_0 is an indenter constant of 2.15 in the present experiment used a diamond pyramid indenter. It was confirmed that the relation between P (245 mN–9.8 N) and a given by Equation 1, i.e. $a \propto P^{1/2}$, is well hold in the present glasses. It was also confirmed that Vickers-produced fracture patterns for the present glasses were radial cracks. The evaluated values of Vickers hardness at room temperature in air are shown in Table II and Fig. 1. It is seen that the Vickers hardness decreases rapidly from 4.5 GPa for the glass with $x = 20$ to 2.9 GPa for the glass with $x = 60$ with the substitution of Bi_2O_3 for B_2O_3. This compositional trend is consistent with that of the glass transition temperature. The Vickers hardness data, therefore, indicate again that Bi–O chemical bonds in

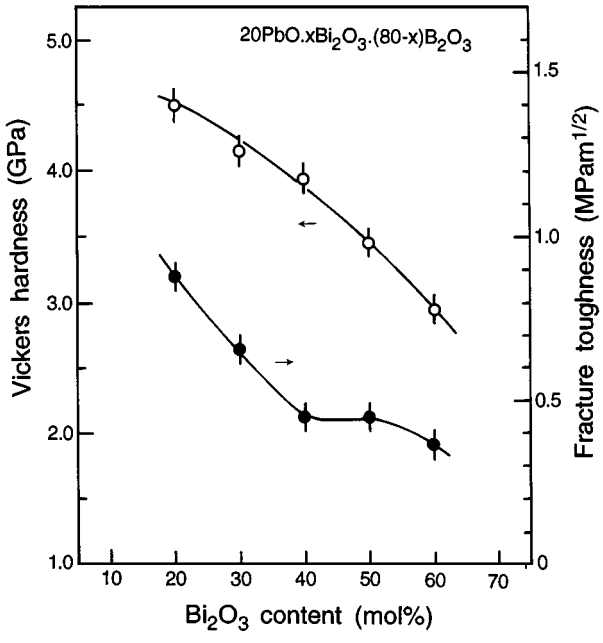

Figure 1 Values of Vickers hardness H_v(○) and fracture toughness K_c (●).

PbO-Bi_2O_3-B_2O_3 glasses are considerably weak. As a comparison, the Vickers hardness values of a tellurite glass of $15Na_2O \cdot 15ZnO \cdot 70TeO_2$ and soda-lime silicate glass ($14Na_2O \cdot 13CaO \cdot 73SiO_2$) reported in previous papers [17, 24] are given in Table II. Tellurite glasses have been considered as promising materials for use in broadband optical amplifier or nonlinear optical devices as similar to Bi_2O_3-based glasses. Soda-lime silicate glass is a typical one of conventional oxide glasses. The values of T_g, d and V_m for these glasses are given in Table I [17]. The Vickers hardness of $20PbO \cdot 60Bi_2O_3 \cdot 20B_2O_3$ glass is almost the same as that of $15Na_2O \cdot 15ZnO \cdot 70TeO_2$ glass. It should be pointed out that both glasses have similar glass transition temperatures and mean atomic volumes.

The values of characteristic crack length, C, in Vickers indenter tests gives information on the resistance to fracture. Fracture toughness, K_c, which is a measure of the resistance to fracture, is expressed by the following Equation 2:

$$K_c = \frac{P}{\beta_0 C^{3/2}} \tag{2}$$

β_0 is a function of Young's modulus E and hardness H_v, and many models for the estimation of β_0 have been proposed [25]. The following equation has been recommended by Japanese Industrial Standards (JIS) for ceramics [26]:

$$K_c = 0.018\left(\frac{E}{H}\right)^{1/2}\left(\frac{P}{C^{3/2}}\right) \tag{3}$$

Equation 3 is almost the same as that proposed by Anstis *et al*. [27]. It was found that the relation between P and C given by Equations 2 and 3, i.e. $C \propto P^{2/3}$, is well hold in the $20PbO \cdot xBi_2O_3 \cdot (80-x)B_2O_3$ glasses. The values of Young's modulus for the glasses were determined from indentation load-unload/displacement experiments, which will be described later, and are given in Table II. Using such Young's modulus values, the K_c values were determined, and are shown in Table II and Fig. 1. The fracture toughness of these glasses is in the range of 0.37–0.88 MPam$^{1/2}$ decreases rapidly with the substitution of Bi_2O_3 for B_2O_3. It should be pointed out that the fracture toughness of these Bi_2O_3-based glasses is larger than that (~0.23 MPam$^{1/2}$) of tellurite glasses [17]. The fracture toughness of the $20PbO \cdot 20Bi_2O_3 \cdot 60B_2O_3$ glass, 0.88 MPam$^{1/2}$, is comparable to that (0.75 MPam$^{1/2}$) of a soda-lime silicate glass [24].

It is noted that the compositional dependence of the fracture toughness in the $20PbO \cdot xBi_2O_3 \cdot (80-x)$ B_2O_3 glasses is not monotonous. That is, the fracture toughness decreases rapidly with the substitution of Bi_2O_3 for B_2O_3 for the glasses with 20–40 mol% B_2O_3, but the glasses with the Bi_2O_3 contents of 40, 50 and 60 mol% show almost a similar fracture toughness of 0.4–0.5 MPam$^{1/2}$. This compositional trend is apparently different from those for glass transition temperature, Vickers hardness or Young's modulus. This behavior might be explained as follows.

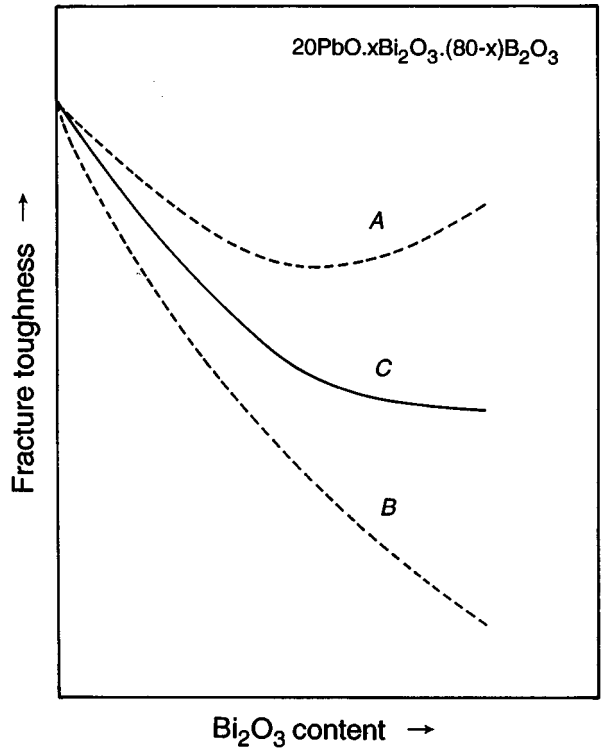

Figure 2 Schematic illustrations of the fracture toughness K_c. (A) Effect of the boron coordination state on K_c, (B) effect of weak Bi–O bonds on K_c, (C) expected net fracture toughness.

Firstly, since Bi−O bonds in the glasses is considered to be weak, the increase of Bi_2O_3 content would cause the decrease of the fracture toughness. It is expected that this effect on the fracture toughness would be monotonous as shown schematically in Fig. 2. Secondly, the change in the boron coordination state in the glasses is not monotonous as described in the Section 3.1. Shinkai *et al.* [28] reported that the fracture toughness of PbO-ZnO-B_2O_3 glasses depends on the boron atom coordination, i.e. the glasses with three coordinated boron atoms show a higher fracture toughness compared with the glasses with four coordinated boron atoms. As suggested by Bartenev *et al.* [29], two-dimensional BO_3 structural units can move more easily without breaking of B–O bonds at the glass transition compared with three-dimensional structural units such as SiO_4. In SiO_2 glass, the viscous fluidity at the glass transition occurs through the thermofluctuation breaking and recomobination of Si–O bonds. Recently, the present authors' group [30] found that copper phosphate glasses with a large amount of Cu^+ (two oxygen coordination) show extremely high resistance against crack formation in Vickers indenter tests compared with the glasses with a large amount of Cu^{2+} (four oxygen coordination). It is expected that in the glasses consisting of low coordination (one- or two-dimensional) structural units, a strain energy given by an indenter would be consumed or relaxed through movements of constituent atoms or structural units themselves toward surrounding open structural spaces. It is also well known that in many crystalline materials fracture surfaces occur along crystallographic cleavage planes of high atomic density. It would be, therefore, reasonable to conclude that the glasses with high BO_4/BO_3 ratios have smaller fracture toughness than that the glasses with low BO_4/BO_3 ratios. It is also expected that the glasses with chain-type (one-dimensional) metaborate groups would have a large fracture toughness. The effect of the change in the boron coordination state on the fracture toughness in the $20PbO \cdot xBi_2O_3 \cdot (80-x)B_2O_3$ glasses would not be monotonous as shown schematically in Fig. 2. Consequently, it is considered that these two factors lead to the compositional dependence of the fracture toughness shown in Table II.

The evaluation of brittleness of glass and ceramics is important for materials design and applications [24, 31–33]. Since brittleness compares deformation to fracture processes, the brittleness, B, defined as the ratio of hardness and the fracture toughness, which was proposed by Lawn and Marshall [31], is used in this study:

$$B = \frac{H}{K_c} \tag{4}$$

The B values for the $20PbO \cdot xBi_2O_3 \cdot (80-x)B_2O_3$ glasses estimated using Equation 4 are given in Table II. The glasses have the values of 5.1–8.6 $\mu m^{-1/2}$, and the $20PbO \cdot 40Bi_2O_3 \cdot 40B_2O_3$ glass shows the largest brittleness. The results indicate that the brittleness is also affected by the boron coordination state and weak Bi−O bond strength. Recently, Sehgal *et al.* [24, 32] have estimated the brittleness for various silicate glasses from the *C/a* ratio obtained in Vickers indentation tests. They reported the values of $B = 5$–$7\ \mu m^{-1/2}$ for soda-lime silicate glasses. The brittleness of $20PbO \cdot xBi_2O_3 \cdot (80-x)B_2O_3$ glasses is, therefore, comparable to soda-lime silicate glasses.

3.3. Temperature dependence of Vickers hardness

The temperature dependences of Vickers hardness of $20PbO \cdot 40Bi_2O_3 \cdot 40B_2O_3$ and $20PbO \cdot 60Bi_2O_3 \cdot 20B_2O_3$ glasses in a vacuum are shown in Fig. 3. It is seen that the hardness decreases almost linearly in the temperature region well below T_g with increasing temperature. The temperature coefficients of the

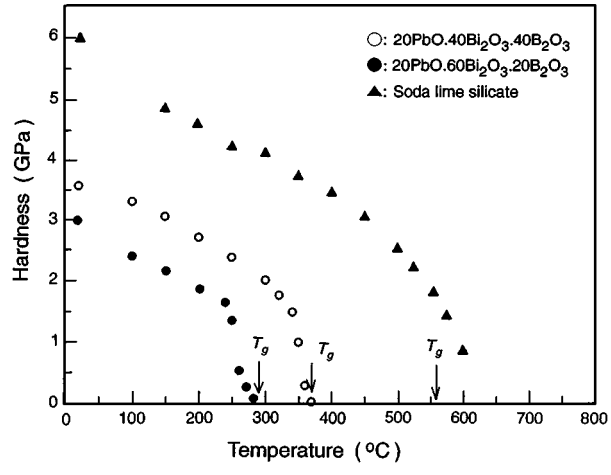

Figure 3 Temperature dependence of Vickers hardness H_v obtained in a vacuum of 1.33×10^{-3} Pa.

hardness in this temperature region dH/dT which were determined from a least square fitting for the data are of -5.67×10^{-3} GPa K^{-1} for the glass with $x = 40$ and of -6.15×10^{-3} GPa K^{-1} for the glass with $x = 60$. Elastic properties are among physical properties which depend on the forces between atoms in solids. As temperature increases, thermal expansion increases the separation between atoms and slightly decreases the forces between atoms, leading to the decrease in elastic modulus with increasing temperature. It is obvious that the decrease in bond strength causes the decreases in hardness. Recently, Watanabe *et al*. [17] reported that the relative change in hardness with temperature for tellurite and soda-lime silicate glasses is closely related to thermal expansion coefficient. Therefore, the data on the temperature coefficient of hardness dH/dT suggest that the bond strength in $20PbO \cdot xBi_2O_3 \cdot (80 - x)B_2O_3$ glasses decreases in an order of -5–-6×10^{-3} GPa K^{-1} with increasing temperature. For some polymers such as polyethylene, it has been demonstrated that the temperature dependence of microhardness is closely related to the thermal expansion coefficient [34, 35].

The Vickers hardness decreases rapidly at and near T_g and is almost zero in the GPa scale at the glass transition. Since the decrease in viscosity causes the increase in deformation under applied stress, the behavior of the temperature dependence of the hardness in the glass transition region shown in Fig. 3 would be closely related to that of the temperature dependence of viscosity. It should be pointed out that the change in the hardness at the glass transition region in the soda- lime silicate is gradual [17]. The "strong" and "fragile" classification concept in glass-forming liquids, introduced by Angell [36], gives new insights for glass transition, structural relaxation phenomenon, glass or supercooled liquid structure and so on. Fragile glass-forming liquids are characterized by non-Arrhenius temperature dependence of shear viscosity in the glass transition region and by generally large heat capacity changes ΔC_p at T_g. That is, in fragile liquids the configurational structure changes steeply with increasing temperature near and above T_g. For example, tellurite glasses belong to the category of fragile liquids [37]. On the other hand, it is well recognized that SiO_2 and GeO_2 are strong liquids because of Arrhenius temperature dependence of viscosity and of small ΔC_p at T_g. SiO_2 and GeO_2 have tetrahedrally coordinated network structures with strong covalent bonds that are expected to experience relatively little disruption during heating. The results shown in Fig. 3, therefore, suggest that $20PbO \cdot 40Bi_2O_3 \cdot 40B_2O_3$ and $20PbO \cdot 60Bi_2O_3 \cdot 20B_2O_3$ glasses with high Bi_2O_3 contents belongs to the category to fragile liquids. That is, bond breakings occur easily at T_g in these glasses, giving easy rearrangements among constituent atoms in the glass transition region.

3.4. Nanoindentation and elastic properties

Fig. 4 shows a schematic load/unload displacement curve for a nonflat indenter with definitions of load P, indentation depth h, the peak indentation load P_{max}, the indenter displacement at peak load h_{max}, the final depth of the contact impression after unloading h_f, and the initial unloading stiffness $S = dP/dh$. The experimentally measured stiffness of the upper portion of the unloading data is expressed by the following Equation 5 [38]:

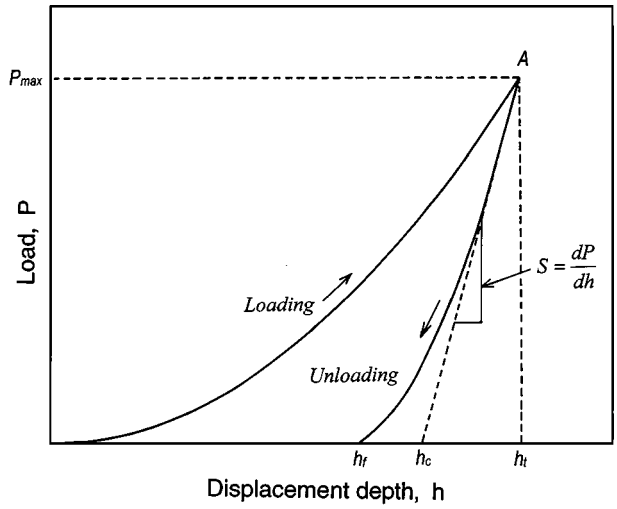

Figure 4 A schemetic load/unload displacement curve in a nonflat indentation experiment for an elastoplastic material. P_{max}: the peak indentation load, h_t: the indenter displacement at peak load, h_f: the final depth of the contact impression after unloading, S: the initial unloading stiffness.

$$S = \frac{dP}{dh} = \frac{2}{\sqrt{\pi}} E_r \sqrt{A} \tag{5}$$

where A is the projected area of indentation (or the contact area) and E_r is a reduced modulus expressed by Equation 6 [38]:

$$\frac{1}{E_r} = \frac{(1 - \nu^2)}{E} + \frac{(1 - \nu_i^2)}{E_i} \tag{6}$$

where E and ν are Young's modulus and Poisson's ratio for the specimen and E_i and ν_i are the same parameters for the indenter. In this study, a diamond Vickers indenter was used, and the elastic parameters for diamond are $E_i = 1140$ GPa and $\nu_i = 0.07$ [39]. When we use the value of the diagonal of the Vickers indentation squared D against A in Equation 5, the following relation is obtained [40].

$$P_{max} = \frac{2E_r D}{\sqrt{2\pi}} (h_f - h_c) \tag{7}$$

Using Equations 6 and 7, Young's moduli for the $20PbO \cdot xBi_2O_3 \cdot (80 - x)B_2O_3$ glasses were evaluated. From a load/unload displacement curve, the fraction of the elastic recovery after finishing unload has been also evaluated. The true hardness H in nanoindentation experiments is derived from the following relation [38]:

$$H = \frac{P_{max}}{A} \tag{8}$$

In this study, the maximum load was 490 mN.

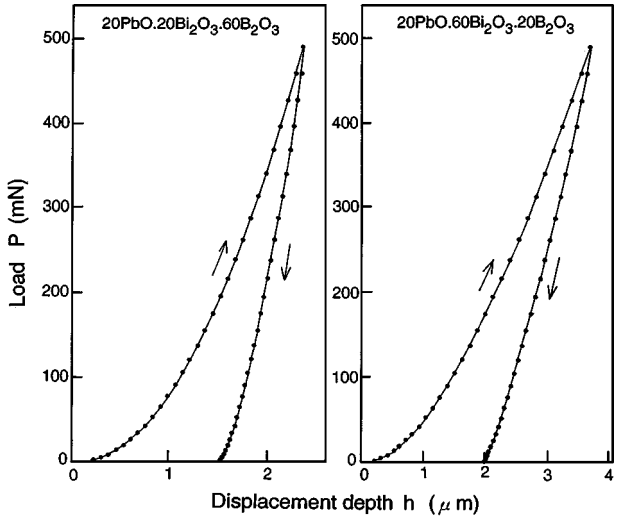

Figure 5 Indenter load versus indenter displacement at room temperature. The maximum load was 490 mN.

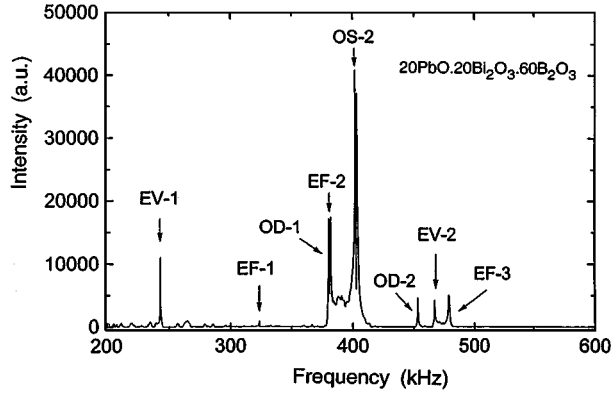

Figure 6 Cube resonance spectrum at room temperature. The corresponding vibration modes are also shown.

The load/unload displacement curves for the $20PbO \cdot xBi_2O_3 \cdot (80-x)B_2O_3$ glasses with $x = 20$ and 60 are shown in Fig. 5, as examples. The cube resonance spectrum for the $20PbO \cdot 20Bi_2O_3 \cdot 60B_2O_3$ glass is shown in Fig. 6, and the Poisson's ratio was determined to be $\nu = 0.27$. This value of $\nu = 0.27$ is almost the same as those ($\nu = 0.27$–0.29) for Bi_2O_3-B_2O_3 glasses with Bi_2O_3 contents of 25.6–56.8 mol% reported by Sanditov and Sangadiev [8]. It is well known that Poisson's ratio in oxide glasses is 0.2–0.3 and is not so sensitive to glass composition. Therefore, we used the value of $\nu = 0.27$ for the $20PbO \cdot xBi_2O_3 \cdot (80-x)B_2O_3$ glasses and evaluated Young's moduli E for the glasses from Equation 6. The evaluated values of H, E_r and elastic recovery are shown in Table II and Fig. 7. It is seen that the fractions of the elastic recovery for the glasses with $x = 20$–50 are 43–45% irrespective of Bi_2O_3 content. The glass with 60 mol% Bi_2O_3 shows the elastic recovery of about 55%. These results indicate that the deformation of the present glasses during indentation loading comprises about 45% elastic deformation and about 55% plastic deformation. Both Young's modulus (24.4–72.6 GPa) and true hardness (1.5–3.8 GPa) decreases monotonously with increasing Bi_2O_3 content. The values of the true hardness evaluated from nanoindentation experiments is much small compared

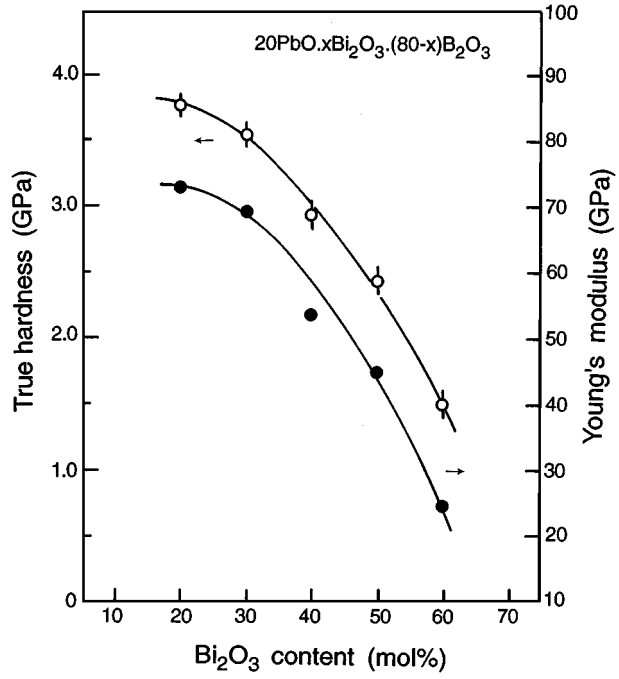

Figure 7 Values of Young's modulus E (●) and true hardness H (○) obtained by nanoindentation tests.

with those of Vickers hardness because of the presence of about 45% elastic deformation, as shown in Table II. In the $20PbO \cdot xBi_2O_3 \cdot (80-x)B_2O_3$ glasses, the true hardness and elastic modulus decrease monotonously with increasing Bi_2O_3 content. This compositional dependence is well consistent with that of glass transition temperature and mean atomic volume. The data obtained in the nanoindentation tests, demonstrate again that Bi−O bonds in the $20PbO \cdot xBi_2O_3 \cdot (80-x)B_2O_3$ glasses are much weaker than B−O bonds and movements of the constituent atoms or structural units during Vickers indenter loading become easily with increasing Bi_2O_3 content. The study of the effect of the maximum load on the elastic recovery in the glasses is now under consideration, which will give more detailed information about the relationship between deformation behaviors and the glass structure.

4. Conclusions

In this study, the hardness and elastic properties of $20PbO \cdot xBi_2O_3 \cdot (80-x)B_2O_3$ glasses with $x =$ 20–60 were evaluated through usual Vickers indentation and nanoindentation tests for the first time. The Vickers hardness, true hardness and Young's modulus decreased monotonously with increasing Bi_2O_3 content. The elastic recovery after unloading was about 45% for the glasses with $x = 20$–50. These compositional trends demonstrate that the strength of Bi–O bonds in these glasses is considerably weak compared with B–O bonds and plastic deformations under indentation loading occur easily. The fracture toughness is strongly affected by the boron coordination states. It was suggested from the temperature dependence of Vickers hardness that the glasses with high Bi_2O_3 contents belong to the category to fragile glass-forming liquids, because the hardness decreased rapidly at and

near the glass transition temperature. The data obtained in the present study will be valuable for technical applications of Bi_2O_3-based glasses in photonics.

Acknowledgements

This work was supported by a Grant of The Sumitomo Foundation and the Grant-in-Aid for Scientific Research from the Ministry of Education, Science, Sports and Culture, Japan. The authors thank Prof. Kozo Ishizaki, Nagaoka University of Technology, for the use of high-temperature type Vickers hardness.

References

1. W. H. DUMBAUGH, *Phys. Chem. Glasses* **27** (1986) 119.
2. H. NASU, T. ITO, H. HASE, J. MATSUOKA and K. KAMIYA, *J. Non-Cryst. Solids* **204** (1996) 78 .
3. N. SUGIMOTO, H. KANBARA, S. FUJIWARA, K. TANAKA and K. HIRAO, *Opt. Lett.* **21** (1996) 1637.
4. K. TERASHIMA, T. H. SHIMOTO and T. YOKO, *Phys. Chem. Glasses* **38** (1997) 211.
5. S. TANABE, K. HIRAO and N. SOGA, *J. Non-Cryst. Solids* **122** (1990) 79.
6. Y. G. CHOI and J. HEO, *ibid.* **217** (1997) 199.
7. A. I. RABUKHIN and G. V. BELOUSOVA, *Glass and Ceramics* **49** (1992) 5.
8. D. S. SANDITOV and S. SH. SANGADIEV, *Glass. Phys. Chem.* **24** (1998) 525.
9. D. M. MARSH, *Proc. Roy. Soc. London* **282A** (1964) 33.
10. J. E. NEELY and J. D. MACKENZIE, *J. Non-Cryst. Solids* **3** (1968) 603.
11. S. M. WIEDERHORN, *J. Amer. Ceram. Soc.* **52** (1969) 99.
12. K. W.PETER, *J. Non-Cryst. Solids* **5** (1970) 103.
13. C. R. KURKJIAN, G. W. KAMMLOTT and M. M. CHAUDHRI, *J. Amer. Ceram. Soc.* **78** (1995) 737.
14. N. SOGA, *J. Non-Cryst. Solids* **52** (1982) 365.
15. J. H. WESTBROOK, *Phys. Chem. Glasses* **1** (1960) 32.
16. N. KOMINE, Y. KAWASE and A. OBARA, *Bull. Electrotech. Laboratory (Japan)* **27** (1963) 919.
17. T. WATANABE, Y. BENINO, K. ISHIZAKI and T. KOMATSU, *J. Ceram. Soc. Japan* **107** (1999) 1140.
18. H. H. DEMAREST, JR, *J. Acous. Soc. Am.* **49** (1971) 768.
19. T. GOTO and N. SOGA, *J. Ceram. Soc. Japan* **91** (1983) 35.
20. C. STEHLE, C. VIRA, D. HOGAN, S. FELLER and M. AFFATIGATO, *Phys. Chem. Glasses* **39** (1998) 83.
21. F. MIYAJI and S. SAKKA, *J. Non-Cryst. Solids* **134** (1991) 77.
22. M. JANEWICZ, J. WASYLAK and E. CZERWOSZ, *Phys. Chem. Glasses* **35** (1994) 169.
23. B. N. MEERA and J. RAMAKRISHNA, *J. Non-Cryst. Solids* **159** (1993) 1.
24. J. SEHGAL and S. ITO, *J. Amer. Ceram. Soc.* **81** (1998) 2485.
25. C. B. PONTON and R. D. RAWLINGS, *Mater. Sci. Tech.* **5** (1989) 865.
26. *Japanese Industrial Standards, Report* 1607, 1990, p. 7.
27. G. R. ANSTIS, P. CHANTIKUL, B. R. LAWN and D. B. MARSHALL, *J. Amer. Ceram. Soc.* **64** (1981) 533.
28. N. SHINKAI, R. C. BRADT and G. E. RINDON, *ibid.* **65** (1982) 123.
29. G. M. BARTENEV, V. A. LOMOVSKOI, G. M. SINITSYNA and A. G. BARTENEVA, *Glass Phys. Chem.* **25** (1999) 390.
30. T. WATANABE, T. MIURA and T. KOMATSU, unpublished data.
31. B. R. LAWN and D. B. MARSHALL, *J. Amer. Ceram. Soc.* **62** (1979) 347.
32. J. SEHGAL, Y. NAKAO, H. TAKAHASHI and S. ITO, *J. Mater. Sci. Lett.* **14** (1995) 167.
33. A. R. BOCCACCINI, *ibid.* **15** (1996) 1119.
34. F. J. B. CALLEJA, C. S. CRUZ, A. G. ARCHE and E. L. CABARCOS, *J. Mater. Sci.* **27** (1992) 2124.
35. F. J. B. CALLEJA, A. F. F. ANIA and D. C. BASSETT, *ibid.* **35** (2000) 1315.
36. C. A. ANGELL, *J. Non-Cryst. Solids* **131/133** (1991) 13.
37. T. KOMATSU, T. NOGUCHI and R. SATO, *J. Amer. Ceram. Soc.* **80** (1997) 1327.
38. W. C. OLIVER and G. M. PHARR, *J. Mater. Res.* **7** (1992) 1564.
39. R. Y. LO and D. B. BOGY, *ibid.* **14** (1999) 2276.
40. J. L. LOUBET, J. M. GEORGES and G. MEILLE, in "Microindentation Techniques in Materials Science and Engineering" edited by P. J. Blau and B. R. Lawn (ASTM STP 889, 1986) p. 72.

Received 6 July
and accepted 27 November 2000